

# Switchable Fresnel lens using polymer-stabilized liquid crystals

Yun-Hsing Fan, Hongwen Ren, and Shin-Tson Wu

School of Optics/CREOL, University of Central Florida, Orlando, Florida 32816

[swu@mail.ucf.edu](mailto:swu@mail.ucf.edu)

<http://lcd.creol.ucf.edu>

**Abstract:** A switchable Fresnel zone plate lens is demonstrated using a polymer-stabilized liquid crystal. The fabrication process is relatively simple and the device can be operated below 10 volts with fast response time. Such a device works well for a linearly polarized light.

©2003 Optical Society of America

OCIS codes: (160.3710) Liquid crystals; (050.1970) Diffractive optics; (160.5470) Polymers

---

## References and links

1. G. Williams, N. J. Powell, A. Purvis and M.G. Clark, "Electrically controllable liquid crystal Fresnel lens," Proc. SPIE **1168**, 352-357 (1989).
2. J. S. Patel and K. Rastani, "Electrically controlled polarization-independent liquid-crystal Fresnel lens arrays," Opt. Lett. **16**, 532-534 (1991).
3. M. Ferstl and A. Frisch, "Static and dynamic Fresnel zone lenses for optical interconnections," J. Mod. Opt. **43**, 1451-1462 (1996).
4. S. Sato, "Liquid-crystal lens-cells with variable focal length," Jpn. J. Appl. Phys. **18**, 1679-1684 (1979).
5. Nabeel A. Riza and Michael C. DeJule, "Three-terminal adaptive Nematic liquid-crystal lens device," Opt. Lett. **19**, 1013-1015 (1994).
6. A. F. Naumov, M. Yu. Loktev, I. R. Guralnik, and G. Vdovin, "Liquid-crystal adaptive lenses with modal control," Opt. Lett. **23**, 992-994 (1998).
7. Werner Klaus, Masafumi Ide, Yutaka Hayano, Shigeru Morokawa, and Yoshinori Arimoto, "Adaptive LC lens array and its application," SPIE **3635**, 66-69 (1999).
8. A. F. Naumov, G. D. Love, M. Yu. Loktev, and F. L. Vladimirov, "Control optimization of spherical modal liquid crystal lenses," Opt. Express **4**, 344-352 (1999).
9. Vladimir V. Presnyakov, Karen E. Asatryan, and Tigran V. Galstian, "Polymer-stabilized liquid crystal for tunable microlens applications," Opt. Express **10**, 865-870 (2002).
10. N. Kitaura, S. Ogata, and Y. Mori, "Spectrometer employing a micro-Fresnel lens," Opt. Eng. **34**, 584-588 (1995).
11. E. Skudrzyk, *The foundation of acoustics* (Springer-Verlag, 1971).
12. F. Sobel, L. Wentworth, and J. C. Wiltse, "Quasi-optical surface waveguide and other components for the 100-to 300-Ge region," IRE Trans. Microw. Tech. **9**, 512-518 (1961).
13. L. Mingtao, J. Wang, L. Zhuang, and S. Y. Chou, "Fabrication of circular optical structures with a 20 nm minimum feature size using nanoimprint lithography," Appl. Phys. Lett. **76**, 673-675 (2000).
14. J. Canning, K. Sommer, S. Huntington, and A. Carter, "Silica-based fiber Fresnel lens," Opt. Comm. **199**, 375-381 (2001).
15. H. Dammann, "Blazed synthetic phase-only holograms," Optik **31**, 95-104 (1970).
16. H. Ren, Y. H. Fan, and S. T. Wu, "Prism grating using polymer-stabilized nematic liquid crystal," Appl. Phys. Lett. **82**, 3168-3170 (2003).

---

## 1. Introduction

Liquid crystal is a very good candidate for electrically switchable lens devices. Various LC lens devices have been reported [1-9] wherein the Fresnel zone plates are more attractive devices due to its focusing abilities and compactness [10]. The Fresnel lenses are suitable for diverse applications in optics, acoustics [11], microwave, and millimeter-wave devices [12].

Both static and electrically switchable Fresnel lenses have been reported [1-3, 10-14]. Methods for fabricating the static Fresnel zone lens are usually based on the lithographic or etching techniques [13, 14]. For the dynamic Fresnel lens, the optical phase elements using a liquid crystal have been described using patterned electrodes and Fresnel structure on quartz substrate [1, 3]. The binary Fresnel patterns are generated by electron beam lithography. Another technique is to make the two neighboring zones with orthogonal LC directors [2]. However, those devices are difficult to be fabricated. In this paper, we demonstrated a Fresnel lens using polymer stabilized liquid crystal (PSLC). The fabrication procedure is relatively simple and the device can be operated below 10 volts with fast response time. Such a device works well for a linearly polarized light. This device has the potential for long focal length and large aperture size.

## 2. Fabrication method

The key element for fabricating the Fresnel zone plate is a patterned photomask that was produced by etching a chromium oxide layer using electron beam lithography. Figure 1 depicts a simplified zone plate pattern and the corresponding LC molecular orientations in the voltage-off state. The innermost zone has radius  $r_1=0.5$  mm and the  $n^{\text{th}}$  zone has radius  $r_n$  which satisfies  $r_n^2 = nr_1^2$ ;  $n$  is the zone number. Our zone plate consists of 80 concentric rings within 1cm diameter. During UV (Loctite model 98016) exposure, the photomask was in proximity contact with the LC cell. As shown in Fig. 1, the odd zones are transparent and even zones are opaque. Thus, polymerization process would first take place in the odd zones resulting in a higher polymer concentration and higher threshold voltage ( $V_{\text{th}}$ ). Although even zones are opaque, monomers could still diffuse to these regions. Therefore, we further cured the cell with a weaker UV light after the photomask had been removed. The even zones have a lower polymer concentration so that their threshold voltage is lower. An LC polymer network replicating zone plate configuration is thus formed.

To fabricate LC zone plate, we mixed 5% UV curable monomer bisphenol-A-dimethacrylate in a LC host (Merck MLC-6252,  $\Delta n=0.078$ ). This monomer has a rod-like structure with a carbon-carbon double bond at both ends. The LC/monomer mixture was injected to a homogeneous cell composing of ITO (indium-tin-oxide)-coated glass substrates. The inner surfaces of the ITO-glass substrates were coated with thin polyimide layers and rubbed in anti-parallel directions. The pretilt angle is  $\sim 3^\circ$  and cell gap is  $d\sim 5\mu\text{m}$ . During exposure, the cell was in proximity contact with the photomask. The UV light with intensity  $I\sim 40$  mW/cm<sup>2</sup> was used to cure the cell from the photomask side for 15 minutes. The photomask was then removed and exposure ( $I\sim 20$  mW/cm<sup>2</sup>) continued for another 15 minutes.

## 3. Experimental results

The prepared polymer-stabilized LC sample is highly transparent in the voltage-off state. Figure 1 shows the schematic diagram illustrating the LC director arrangements of the polymer-stabilized LC Fresnel zone plate. In the low voltage regime, the LC molecules in the even zones are reoriented first while the molecules in the odd zones remain in the original alignment owing to their higher threshold voltage. A binary-phase Fresnel lens is thus formed. If the polarization of the incident light is parallel to the rubbing direction of the cell, the phase difference between the neighboring zones is  $\phi = 2\pi\delta n d/\lambda$ , where  $\delta n$  is the difference of the effective refractive indices in the adjacent zones,  $d$  is the cell gap, and  $\lambda$  is the wavelength of the incident beam. The induced phase shift is electrically tunable. The phase change corresponds to color change when observed from an optical microscope through crossed polarizers. Under this visual inspection, the rubbing direction of the LC cell was oriented at  $45^\circ$  with respect to the optical axis of the linear polarizer. The optical micrographs of the PSLC Fresnel lens were taken at different voltages. Results are shown in Fig. 2.

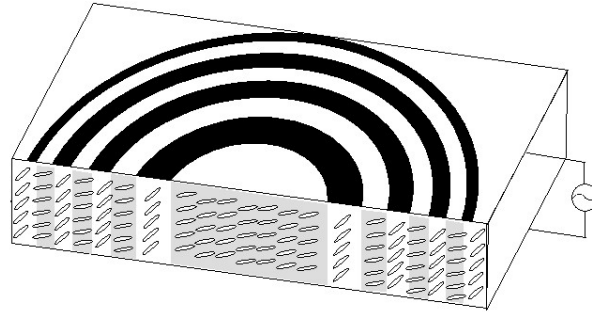


Fig. 1. Schematic representation of the photomask patterns and the corresponding LC arrangement of the PSLC Fresnel lens.

Figures 2(a-d) show a portion of the LC zone plate at  $V=0, 4, 7$  and  $10 V_{\text{rms}}$ , respectively. At  $V=0$ , the sample is optically homogeneous across the entire zone plate. As the voltage exceeds a threshold ( $\sim 1.8 V_{\text{rms}}$ ), the Fresnel zone starts to appear, as shown in Figs. 2(b-d). The color change of the odd and even zones results from the refractive index change. In the higher voltage regime ( $\sim 46 V_{\text{rms}}$ ), the bulk LC directors are orientated nearly perpendicular to the substrates, thus the zone structure is gradually erased. A drawback of the PSLC Fresnel lens is that it is polarization sensitive. For the light polarization perpendicular to the rubbing direction, it encounters the ordinary refractive index  $n_o$  of the liquid crystal layer. To overcome the polarization dependence, stacking two orthogonal homogeneous PSLC zone plates could be considered.

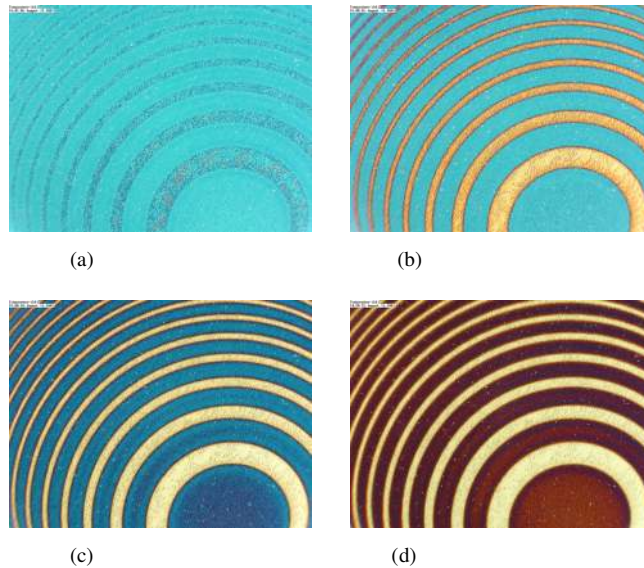


Fig. 2. Microscope images of the PSLC cell at (a)  $V=0$ , (b)  $4 V_{\text{rms}}$ , (c)  $7 V_{\text{rms}}$ , and (d)  $10 V_{\text{rms}}$ . The LC cell is sandwiched between crossed polarizers.

For a binary-phase Fresnel lens, the primary focal length  $f_1$  is related to the innermost radius  $r_1$  as  $f_1 = r_1^2 / \lambda$ . The primary focal length of our LC Fresnel lens was estimated to be 50 cm for the He-Ne laser employed ( $\lambda=632.8$  nm). Due to the higher-order Fourier components, Fresnel zone lens normally has multiple foci at  $f, f/3, f/5, \dots$ , but most of light

diffraction into the primary focus. The diffraction efficiency ( $E_n$ ) of these foci is  $E_n = \text{sinc}^2(n/2)$ ,  $n = \pm 1, \pm 3, \pm 5, \dots$ . Therefore, the theoretical diffraction efficiency of the primary focus is 41% [15]. However, the diffraction efficiency of our photomask was measured to be only 25.6%, which is lower than the theoretical value of binary-phase structure because all the even zones are opaque.

Figure 3 shows the experimental setup for studying the focusing properties of the PSLC Fresnel zone plate. The output beam of the He-Ne laser was magnified by two convex lenses with the focal lengths 50 mm and 250 mm. A pinhole with 30  $\mu\text{m}$  diameter was put at the focal point of the first lens serving as a spatial filter. The beam diameter was expanded to  $\sim 1$  cm just to cover the aperture of the zone patterns. A sheet polarizer was used with its optical axis parallel to the cell rubbing direction. Light focusing properties of the cell was measured using a CCD camera (SBIG Model ST-2000XM) connected to a computer. The CCD camera was set at a distance of 50 cm from the PSLC Fresnel lens.

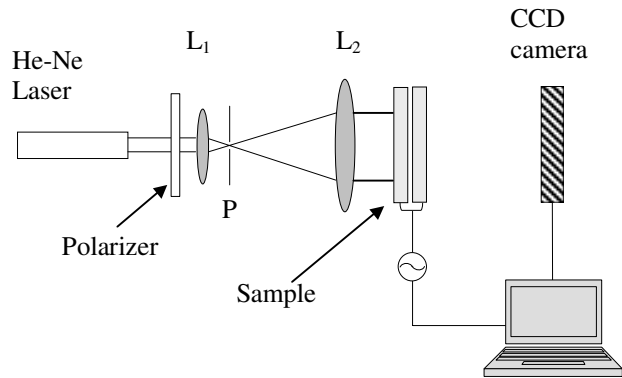


Fig. 3. The experimental setup for studying the focusing properties of the PSLC Fresnel lens.  $L_1$ : focal length 50 mm,  $L_2$ : focal length 250 mm, and P: 30  $\mu\text{m}$  pinhole.

Figure 4 shows the focusing property of the PSLC Fresnel lens displayed from the CCD camera. In the absence of sample, the laser beam has a Gaussian beam profile shown in Fig. 4(a). When the sample is present and  $V=0$ , the PSLC lens possesses a small focusing effect, as shown in Fig. 4(b). This is due to the different polymer concentration between odd and even zones which makes the effective refractive indices slightly different between the adjacent zones. At  $V=8 V_{\text{rms}}$ , the focusing effect is intensified, as shown in Fig. 4(c).

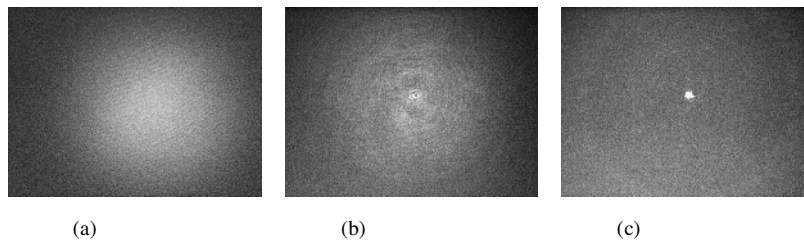


Fig. 4. The observed laser beam images: (a) without LC sample, (b) with sample at  $V=0$ , and (c) with LC sample at  $8 V_{\text{rms}}$ .  $\lambda=633$  nm.

Figure 5 shows the image quality of the PSLC Fresnel lens using a transparent alphabet M placed between lens  $L_2$  and sample. The CCD camera was located at  $\sim 27$  cm from the sample. At  $V=0$ , an image of "M" with the original size was recorded by CCD, as shown in Fig. 5(a).

When  $8 V_{\text{rms}}$  was applied to the lens, the image “M” was obviously shrunken, as shown in Fig. 5(b).

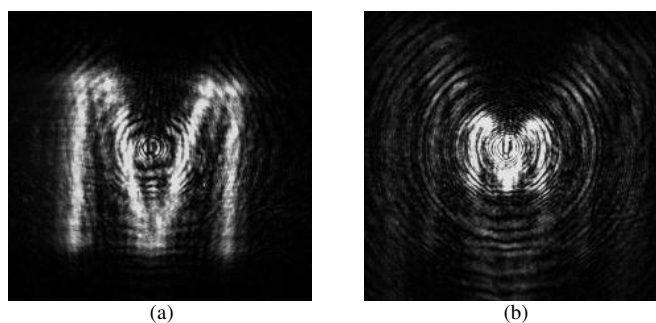


Fig. 5. The observed laser beam images (a) at  $V=0$  and (b) at  $8 V_{\text{rms}}$ .  $\lambda=633$  nm. The CCD camera was 27 cm away from the sample

Figure 6 shows a representative example of the measured three-dimensional intensity distribution at the primary focal point of the LC Fresnel lens. At  $8 V_{\text{rms}}$ , a sharp focal spot was observed. Figure 7 plots the measured laser intensity profiles at different voltages. In the voltage-off state, a slight focusing effect exists. At  $V=8 V_{\text{rms}}$ , the peak intensity occurs. As the voltage continues to increase (say,  $V=20 V_{\text{rms}}$ ), the peak intensity decreases.

Due to the polymer network effect [16], the PSLC Fresnel lens has fast response time. The rise and decay time were measured between 0 and  $8 V_{\text{rms}}$  and results are 4.4 and 9.1 ms, respectively, for the  $5\text{-}\mu\text{m}$  PSLC (5 wt% monomer) Fresnel lens. Increasing monomer concentration would lead to a stronger anchoring force between the polymer network and LC interfaces. As a result, the response time can be even faster. The tradeoff is that the required operating voltage increases proportionally.

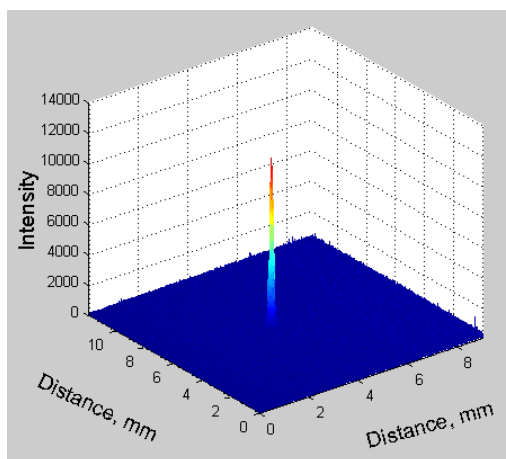


Fig. 6. Beam intensity profile measured by the CCD camera at  $V=8V_{\text{rms}}$ . The diameter of the Fresnel zone plate is 1 cm and the focal length is 50 cm.

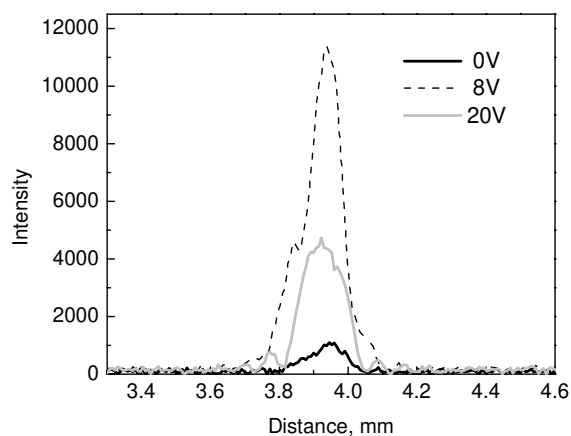


Fig. 7. Beam intensity profiles at (a)  $V=0$ , (b)  $8 V_{rms}$ , and (c)  $20 V_{rms}$ . The diameter of the Fresnel zone plate is 1 cm and the focal length is 50 cm.

Figure 8 shows the measured diffraction efficiency as a function of the applied voltage. The maximum diffraction efficiency is approximately 23%. This value is close to the diffraction efficiency of 25.6% for the photomask alone. The slightly lower diffraction efficiency might be due to the defects of the polymer network at the zone edges, which results in molecular disorder. A small light scattering was observed at the zone edges.

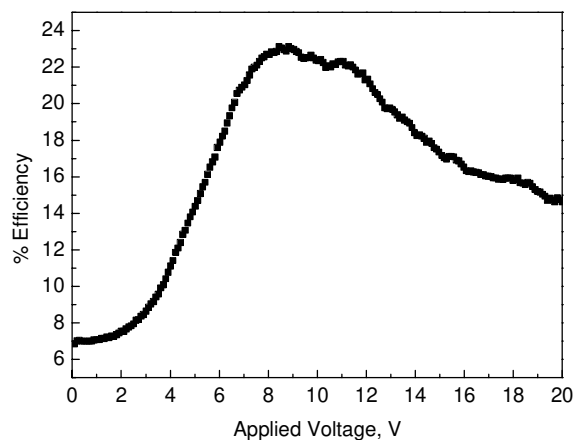


Fig. 8. The voltage-dependent diffraction efficiency of the PSLC Fresnel lens. LC: MLC-6252, cell gap  $d=5 \mu\text{m}$ , and monomer concentration 5%.

#### 4. Conclusion

In conclusion, we have demonstrated a switchable Fresnel lens using polymer stabilized liquid crystals. The fabrication process is relatively simple. The focusing behavior of the PSLC Fresnel lens can be controlled by a homogeneous electric field. The required operating voltage is below 10 V<sub>rms</sub> and response time is around 5 ms.

The authors are indebted to Mr. Yi-Pai Huang (National Chiao Tung University, Taiwan) for designing the photomask. This work is supported by DARPA under Contract No. DAAD19-02-1-0208.